

Article

Drug Release Kinetics of PLGA-PEG Microspheres Encapsulating Aclacinomycin A: The Influence of PEG Content

Mariana Sousa Costa, Ana M. Ramos and M. Margarida Cardoso * 

LAQV-REQUIMTE, Departamento de Química, Nova School of Science and Technology | NOVA FCT, Universidade NOVA de Lisboa, Quinta da Torre, 2829-516 Caparica, Portugal; marianafscosta@gmail.com (M.S.C.); ana.ramos@fct.unl.pt (A.M.R.)

* Correspondence: margarida.cardoso@fct.unl.pt

Abstract: The present study evaluates the effect of PEG content on the characteristics of poly(lactic-co-glycolic acid)-polyoxyethylene (PLGA-PEG) microspheres loaded with a small molecular weight drug on the polymer matrix degradation behavior of the polymeric matrix and drug release profile. Aclacinomycin A (ACM) was encapsulated in PLGA-PEG microspheres with varying PEG content (0%, 5%, 10%, or 15%) using the oil-in-water solvent evaporation method. Microspheres were obtained with sizes ranging from 45–70 nm, drug loading around 1.3% and encapsulation efficiencies between 48–70%. The produced microspheres were further characterized in terms of degradation behavior and drug release kinetics. The results showed that while PEG content had minimal impact on drug loading and microsphere size, it significantly influenced the degradation behavior of the microspheres and its weight in the release process. In vitro drug release profiles exhibited a three-phase pattern for all PLGA-PEG microspheres with faster and more extensive ACM release compared to PLGA microspheres, being the release improved with the PEG content increase. The Corrigan model was successfully applied to the release data yielding burst-phase kinetic constants (k_b) between 0.082–0.288 and degradation/erosion kinetic constants (k) between 0.054–0.093 day⁻¹, both of which increased with higher PEG content.

Keywords: PLGA-PEG copolymers; biodegradable polymers; controlled release; polymeric microparticles; polymer degradation; aclacinomycin release



Academic Editor: Paolo Trucillo and Yi Lu

Received: 30 September 2024

Revised: 20 November 2024

Accepted: 24 December 2024

Published: 4 January 2025

Citation: Costa, M.S.; Ramos, A.M.; Cardoso, M.M. Drug Release Kinetics of PLGA-PEG Microspheres Encapsulating Aclacinomycin A: The Influence of PEG Content. *Processes* **2025**, *13*, 112. <https://doi.org/10.3390/pr13010112>

Copyright: © 2025 by the authors. Licensee MDPI, Basel, Switzerland. This article is an open access article distributed under the terms and conditions of the Creative Commons Attribution (CC BY) license (<https://creativecommons.org/licenses/by/4.0/>).

1. Introduction

Anti-cancer drugs often cause undesirable toxic effects, making the control of dosage, release rate, and targeted delivery as crucial as drug discovery itself for clinical success. Biodegradable microspheres have demonstrated potential to release a broad variety of molecules, particularly via parenteral routes, enhancing therapeutic efficacy through controlled and sustained release over time [1].

Several polymers have been explored for drug delivery systems in the pharmaceutical industry. Among them, aliphatic polyesters such as polylactide (PLA), polyglycolide (PGA), and especially their copolymers like PLGA, approved by the U.S. Food and Drug Administration (FDA), have generated great interest due to their excellent biocompatibility, biodegradability, and mechanical strength [2–5]. Their commercial availability in different molecular weights, copolymer ratios, stereochemistry, and co-monomer sequences, combined with their capacity to control particle size, drug loading and porosity, enables the design of diverse drug release profiles [6–9]. Drug release from biodegradable PLGA

microspheres is usually driven by a combination of drug diffusion and hydrolysis and degradation of the polymer material [9].

Incorporating PEG into biodegradable polyesters introduces hydrophilicity into the polymers. These hydrophilic segments act as a “water pump” [10], thereby promoting polymer degradation and facilitating drug release from microparticles (MP) [7–16]. Phase image TM-AFM analysis showed that the PEG chains were mostly located on the surface of nanoparticles of poly(lactic acid) (PLA) and PEG [17], which promoted water infiltration into the nanoparticles [14]. Microscopy studies show that the penetration rate of water increases in PLGA-PEG triblock MP compared to PLGA [18]. Yeh et al. observed a significant alteration in the release profile having obtained a 4-fold increase in the amount of ovalbumin release from the polymer matrix in microspheres produced with PLGA and PEG blends compared to PLGA alone [19]. Also, Lochmanann et al. have verified that higher PEG contents produce substantially higher release rates of a growth factor (rhBMP-2) from PLGA-PEG MP [13]. Additionally, the biocompatibility of the delivery system can be improved, as it correlates directly with the degree of surface hydrophilicity [20]. PLGA-PEG copolymer-based MPs have been widely studied, with research examining the impact of factors such as drug loading [21–23], drug structure and size [23], particle size [24], and polymer molecular weight [7,25] on drug release. The molecular structure of PLGA-PEG is shown in Figure 1A.

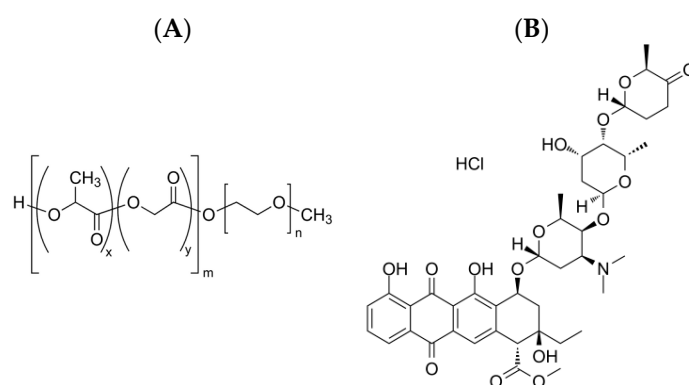


Figure 1. Chemical structures of PLGA and PLGA-PEG polymers (A) and aclacinomycin (B).

While the effect of PEG content on drug encapsulation and release from MP loaded with high molecular weight molecules, such as peptides and proteins, has been extensively studied [10,13,18,19,26], limited research has explored its impact on low molecular weight drugs [27]. Notably, the structure and molecular weight has been shown to significantly influence microparticle characteristics and drug release kinetics [23]. Therefore, the purpose of our study is to prepare PLGA-PEG MP with varying PEG contents, loaded with a low molecular weight drug, using the oil-in-water emulsion evaporation method. We seek to evaluate how the PEG content within the polymeric matrix influences the degradation of the microparticles and the release profile of low molecular weight drugs. As it was expected that the presence of PEG would increase the degradation/erosion process of the particles, the Corrigan model, which accounts for the contribution of diffusion and polymer degradation/erosion processes, making it possible to describe three-phase release profiles, was chosen from among the various models described in the literature [23] to describe the *in vitro* release data and assess the impact of PEG content on both the drug release kinetics and underlying release mechanisms. The model drug used in this work is Aclacinomycin A (ACM) (chemical structure presented in Figure 1B), an anthracycline antibiotic that is widely applied in cancer treatments particularly for leukemia and certain solid tumors [28,29].

It has poor water solubility but a high affinity for lipids, facilitating its accumulation in cell membranes and tissues. Upon intravenous injection, ACM-A is rapidly metabolized (half-life of 13.3 h) in the liver with biliary excretion being the primary route for elimination. The absence of cross-resistance with other anthracyclines and the reduced level of cardiotoxicity compared to other anthracyclines make ACM a suitable choice for treating neoplasms resistant to previous anthracycline therapies or recurrent cases [30].

2. Materials and Methods

2.1. Materials

Poly(DL-lactide-co-glycolide) (PLGA) (50:50) (Mw 70,000–80,000), Poly (vinyl alcohol) (Mw 30,000–70,000) (PVA), and chloroform $\geq 99.8\%$ purity were purchased from Sigma-Aldrich (St. Louis, MI, USA). Resomer PEG type RGP d5055 (diblock, 5% PEG, Mw $\sim 600,000$) (PLGA-5% PEG), d50105 (diblock, 10% PEG, Mw $\sim 700,000$) (PLGA-10% PEG) and d50155 (diblock, 15% PEG, Mw $\sim 550,000$) (PLGA-15% PEG) were bought from Boehringer Ingelheim (Ingelheim, Germany). Aclacinomycin A was acquired from CalBiochem (Merck KGaA, Darmstadt, Germany). Dichloromethane and acetonitrile (HPLC gradient grade) were purchased from Panreac (Panreac Química, Barcelona, Spain). Methanol ($\geq 99.8\%$ purity) and phosphate buffered saline (PBS) were purchased from Fluka (Buchs, Switzerland). All chemicals were used with no further purification. All experiments with ACM were carried out under subdued light to prevent photodegradation of this drug.

2.2. Microspheres Preparation

Empty and drug-loaded MP were prepared using PLGA and PLGA-PEG containing 5%, 10% and 15% of PEG as polymers by the o/w emulsion solvent evaporation method, schematically represented in Figure 2.

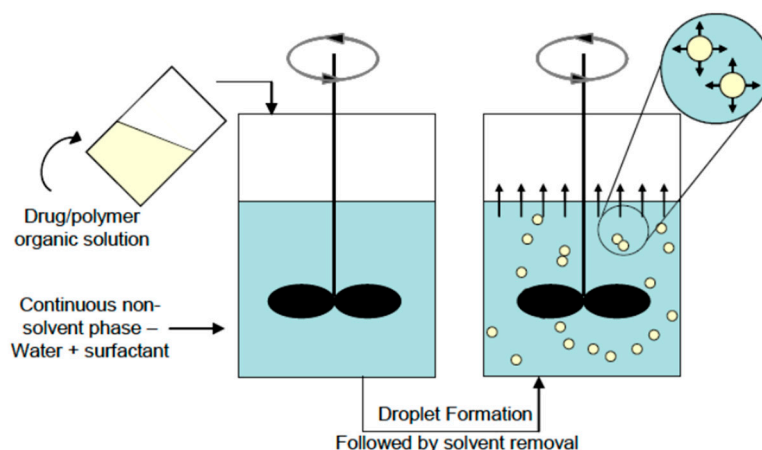


Figure 2. Schematic representation of the solvent extraction/evaporation method.

When preparing drug-loaded MP, 3 mg of ACM dissolved in 0.1 mL of methanol was added to a solution of 150 mg of polymer dissolved in 3 mL of DCM and agitated in a vortex for 1 min. This polymeric solution was then poured into 800 mL of an aqueous solution containing 0.25% w/V PVA, emulsified for 2 h with a two-baffled rotator at 1200 rpm and magnetically stirred for 4 h to ensure complete solvent evaporation and particle solidification. MP were collected by centrifugation at 12,000 rpm (Sartorius, Sigma 4K15, Gottingen, Germany) and washed with deionized water before being freeze-dried (Telstar Cryodos, Barcelona, Spain). The same recipe, without the addition of ACM to the polymer solution, was used to prepare the unloaded microspheres.

2.3. Microsphere Characterization

2.3.1. Morphology

Scanning electron microscopy (SEM) was utilized to assess the surface morphology and estimate the size of the obtained MP. Freeze-dried MP were mounted onto metallic studs and gold coated under an argon atmosphere. The SEM analysis was conducted using a DSM 962 (Zeiss, Germany) microscope at an accelerating voltage of 20 kV.

2.3.2. Particle Size and Size Distribution

Laser diffraction spectrometry (LDS) was used to measure the mean particle size and size distribution of the produced MP in a Coulter LS 130 (Coulter Electronics, Amherst, MA, USA) spectrometer. Prior to measurements freeze-dried MP were dispersed in a surfactant aqueous solution (Coulter Dispersant, Coulter Electronics, Amherst, MA, USA) and sonicated for 1 min at 500 W using a probe. All measurements were performed in triplicate.

2.3.3. Differential Scanning Calorimetry

Thermal analysis of the microspheres was carried out with a differential scanning calorimeter Setaram DSC 131 (Setaram, Newark, CA, USA) 10 mg of MP were placed in sealed aluminum pans and heated, under nitrogen atmosphere, from $-20\text{ }^{\circ}\text{C}$ to $80\text{ }^{\circ}\text{C}$ at a rate of $5\text{ }^{\circ}\text{C}\cdot\text{min}^{-1}$ and from $25\text{ }^{\circ}\text{C}$ to $250\text{ }^{\circ}\text{C}$ at a rate of $10\text{ }^{\circ}\text{C}\cdot\text{min}^{-1}$.

2.3.4. Encapsulation Efficiency and Drug Loading Capacity

A precisely weighed quantity of MP was dissolved in 5 mL of DCM and placed in a desiccator until all the solvent is completely evaporated. After the addition of 10 mL of acetonitrile/acetic buffer (pH 4) 50:50 (v/v) samples were analyzed by HPLC (Hitachi-Merck) using a Merck RP-18 (Merck, Germany) column and a UV detector (Merck Hitachi, Japan) with a wavelength of 229 nm to quantify the drug encapsulated inside the MP. A 50:50 mixture of acetic buffer (pH 4) and acetonitrile was used as the mobile phase at a flow rate of $0.8\text{ mL}\cdot\text{min}^{-1}$.

The encapsulation efficiency of drug was calculated as the percentage of the actual mass of drug encapsulated in MP and the mass of drug added initially during the preparation of MP, according to Equation (1).

$$\text{Encapsulation efficiency(\%)} = \frac{\text{Mass of drug in MP}}{\text{Mass of feed drug}} \times 100 \quad (1)$$

The MP ACM loading was obtained as the percentage of the mass of drug in MP and the mass of MP, as shown in Equation (2).

$$\text{Drug loading(\%)} = \frac{\text{Mass of drug in MP}}{\text{Mass of MP}} \times 100 \quad (2)$$

2.3.5. Polymer Molecular Weight Determination

The polymer average molecular weight in MP was determined at different times of degradation using a size exclusion chromatography (SEC) apparatus (Waters, Milford, MA, USA) and a model 2410 refractive index detector. The analysis was conducted at $30\text{ }^{\circ}\text{C}$, with chloroform serving as the mobile phase. A set of three columns (Waters Ultrastayragel)— 10^3 \AA , 10^4 \AA , and 10^5 \AA —was employed for the analysis after calibration using monodisperse polystyrene (PS) standards with molecular weights ranging from 2×10^3 to 4×10^6 from Waters and Polymer Laboratories. The Mark–Houwink equation $[\eta] = K M^a$, where $[\eta]$ represents the viscosity number limit and K and the Mark–Houwink constants specific to the polymer/solvent/temperature system, was applied to convert the

calibration curve. The values of these constants for poly(DL-lactide) ($K = 0.0074 \text{ mL} \cdot \text{g}^{-1}$; $a = 0.87$) were utilized to determine the molecular weights of PLGA and of various Resomer PEG samples. For the PS/chloroform system, $K = 0.0049 \text{ mL} \cdot \text{g}^{-1}$ and $a = 0.78$ were used [18]. MP were dissolved in chloroform (0.2% w/v) and 150 μL were used as the injection volume.

2.3.6. In Vitro Release Studies

A total of 10 mg of particles were dispersed in 5 mL PBS buffer (pH 7.4) in tubes and placed in a 37 °C horizontal shaker (110 rpm). At specific times, the tubes were centrifuged at 10,000 rpm for 10 min, the supernatant was collected, and the tubes were placed in the incubator after the addition of 5 mL of fresh PBS. The supernatant was analyzed by HPLC to determine the ACM content as described in the encapsulation efficiency section.

2.3.7. In Vitro Particle Degradation Study

In the particle degradation study, unloaded MP were processed as detailed in the in vitro release study. At specific times, the supernatant from the tube was collected after centrifugation at 10,000 rpm for 10 min and fresh medium was replaced except in one tube. The MP of this tube were lyophilized after being washed with distilled water. The morphology of the particles and the polymer average molecular weight were determined.

2.3.8. Calculation Methods

Non-linear regression calculations were performed using the software package Scientist™ (version 2) from Micromath® (Saint Louis, MO, USA), employing both least squares and simplex algorithms with initial parameter estimates provided as starting values. The software generated estimated parameters, 95% confidence intervals, and standard deviations (S.D.). The adequacy of the equation in describing the experimental data was evaluated using the adjusted coefficient of determination (R^2_{adj}) (Equation (3)), and the model selection criterion (MSC) (Equation (4)) which is a modified Akaike Information Criteria, provided by Micromath Scientific Software. This criterion has the advantage of being independent of the magnitude of the y_i . The more appropriate model is that with the larger MSC.

$$R^2_{\text{adj}} = 1 - \frac{(1 - R^2)(n - 1)}{n - p - 1} \quad (3)$$

where R^2 is the sample R squared, n is the number of points and p is the number of independent variables.

$$\text{MSC} = \ln \left(\frac{\sum_{i=1}^n w_i (y_{\text{obs}_i} - \bar{y}_{\text{obs}})^2}{\sum_{i=1}^n (y_{\text{obs}_i} - y_{\text{cal}_i})^2} \right) - \frac{2p}{n} \quad (4)$$

where n is the number of points, p is the number of fitted parameters, w_i is the weight applied to each point and \bar{y}_{obs} is the weighted mean of the observed data.

3. Results and Discussion

3.1. Microsphere Characterization

MP were produced using an emulsion solvent diffusion method. The surface morphology and size of the MP produced prepared using PLGA and three different diblock PLGA-PEG copolymers containing 5% PEG, 10% PEG and 15% PEG were examined by scanning electron microscopy and representative pictures with different scales are shown in Figure 3.

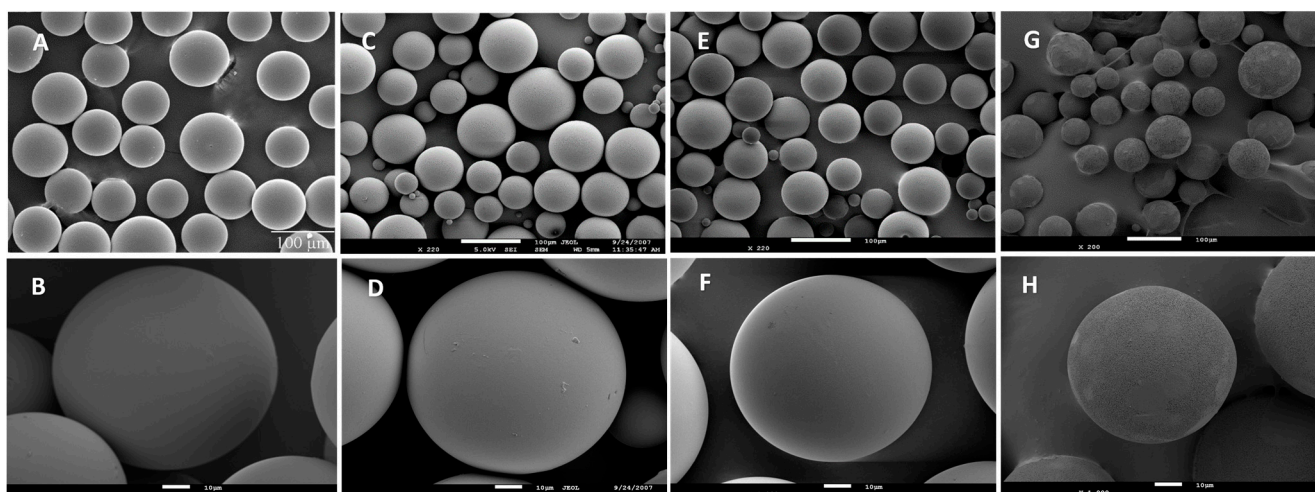


Figure 3. Representative SEM images of prepared MP: PLGA (A,B), PLGA-5% PEG (C,D), PLGA-10% PEG (E,F), PLGA-15% PEG (G, H). The scaling bars correspond to 100 μm (upper panel) and 10 μm (lower panel).

All MP present a spherical shape, while concerning the surface, microspheres made of PLGA and PLGA-co-PEG copolymers with lower percentages of PEG, 5% PEG and 10% PEG (Figure 3A–F), show an apparent smooth surface without visible pores, distinctively different from the porous morphology of those microspheres with a percentage of 15% PEG (Figure 3G,H). This effect may be a result of the increase of the polymer chains' flexibility with the presence of PEG which can improve the diffusion of DCM during the microspheres preparation process causing the formation of pores on the microspheres surface. This increase in flexibility and malleability is confirmed by the decrease in the polymer glass transition temperature (T_g) observed in the DSC thermograms of particles, as shown in Table 1. The data indicate that the incorporation of PEG into the polymeric matrix leads to a reduction in T_g , demonstrating that PEG enhances the flexibility of the polymer. The following linear relation between T_g and PEG content is obtained: T_g ($^{\circ}\text{C}$) = $45.3 - 1.76 \times \% \text{ PEG}$, $r^2 = 0.941$. This reduction is a consequence of its smaller structural unit, less substituted, and involving a lower number of atoms, which is reflected by its thermal characteristics, namely by the low T_g (-22 $^{\circ}\text{C}$) [31].

Table 1. Drug loading, encapsulation efficiency, mean size diameter (MSD) and glass transition temperature (T_g) of ACM loaded microspheres.

PEG Content (%)	Drug Loading (%)	Encapsulation Efficiency (%)	MSD (μm)	T_g ($^{\circ}\text{C}$)	T_g Unloaded ($^{\circ}\text{C}$)
0	1.4 ± 0.2	66 ± 8	44.9 ± 0.6	43.0	40.7
5	1.2 ± 0.1	70 ± 4	48.8 ± 0.9	38.5	37.4
10	1.1 ± 0.2	48 ± 10	58.4 ± 1.0	30.6	28.0
15	1.3 ± 0.1	64 ± 5	70.3 ± 2.0	16.3	13.7

Samples represent the mean \pm SD ($n = 3$) for drug loading, encapsulation efficiency and MSD.

DSC thermograms show no melting point, indicating that PLGA-PEG copolymers, like PLGA, exhibit amorphous structures. As amorphous polymers typically display more uniform and reproducible degradation kinetics [32] these copolymers present a distinct advantage for use in drug delivery systems. No endothermic peak corresponding to the melting of the crystalline drug was visible in the DSC charts of drug loaded microspheres which can signify that the drug is in an amorphous state [33]. The values of the polymer T_g obtained for the loaded microspheres (Table 1) were slightly higher (1–2.6 $^{\circ}\text{C}$) than those

obtained for the unloaded microspheres which, according to Mallardé et al. can indicate a reduction in the polymer chain flexibility due to interactions established between the polymer and the drug [10].

The observed sizes on SEM micrographs of PLGA-PEG microspheres range from 50 μm to 70 μm , in agreement with the sizes measured by laser diffraction spectrometry. A gradual increase in particle size is observed as the PEG content increases with diameters ranging from $44.9 \pm 0.6 \mu\text{m}$ for particles containing no PEG to $70 \pm 2 \mu\text{m}$ for those with 15% PEG. Similar results were reported by Lochmann et al. [13], who attributed them to slower microsphere hardening, allowing more time for coalescence during particle formation.

The values of ACM encapsulation efficiency and loading obtained, presented in Table 1, range between 48–70% and 1.0–1.40%, respectively, showing no evident variation related to the amount of PEG in the polymer. The encapsulation efficiency values obtained are slightly higher than those reported for lower molecular weight molecules such as bendumustine, indomethacin and ketoprofen (32% to 52%) [23,34] and are lower than those reported for PLGA-PEG MP containing peptides and proteins (80% to 95%) [10,13,19,26].

3.2. In Vitro Degradation Study

Microspheres made of PLGA, PLGA-5% PEG, PLGA-10% PEG and PLGA-15% PEG were submitted to the same experiment conditions as for the drug release studies to determine the polymer degradation effects on drug release properties of microspheres. Microspheres degradation was characterized by SEC to determine the alteration in polymer molecular weight and by SEM to determine the change in morphology. Figure 4 displays the evolution of the weight average molecular weight (Mw) with time. The Mw data of the different polymers were normalized to the initial Mw of each polymer to facilitate the analysis. The results show a time-dependent exponential decrease in molecular weight indicating that polymer degradation follows first-order kinetics, as reported in literature [35]. This behavior is characteristic of the hydrolytic chain cleavage of the ester bonds linking lactic acid and glycolic acid units, the primary degradation mechanism for aliphatic polyesters such as PLGA and PEG-PLGA during autocatalytic processes [36]. The polymer degradation products can also plasticize the polymer and increase the osmolality which increases the rate of water absorption and decreases the transport resistance of the polymer [37]. As expected, microspheres made of PLGA present the lowest polymer degradation rate, 0.047 day^{-1} , slightly below reported values in the literature ($0.0657\text{--}0.0759 \text{ day}^{-1}$) for PLGA of comparable molecular weights [7,35,38]. This polymer is the most hydrophobic and does not allow the water in as fast as the polymers containing PEG. In contrast, PLGA-15% PEG microspheres exhibited the highest degradation rate, 0.988 day^{-1} .

Water permeation occurs immediately after immersion in water. The presence of PEG enhances the polymer hydrophilicity allowing more water to diffuse into the polymer matrix. Water molecules have also been reported to have a plasticizing effect on polymers, thus making their chains more flexible and consequently increasing the rate of water permeation. This water absorption accelerates the polymer's hydrolysis reaction, ultimately leading to a reduction in molecular weight (MW) and a decrease in the polymer's hydrophobicity [39,40]. Also, the lowering of the micro pH as a result of the products of the hydrolysis reaction of the polymer will, in turn, accelerate the degradation [18]. These results agree with the morphological changes observed for the different microspheres at various stages during release shown in Figures 5–8. Figures 6 and 7 show that the shape of the microspheres of PLGA-5% PEG and PLGA-10% PEG changed during the incubation period with coalescence becoming apparent after 10 days (Figures 6B and 7B), in contrast to PLGA particles, which consistently maintained their integrity (Figure 5). At this degradation time, the polymer molecular weight had decreased significantly, reaching 10% of its

initial value (Figure 4). As polymer erosion progressed, a more noticeable change occurred (Figures 6C and 7C).

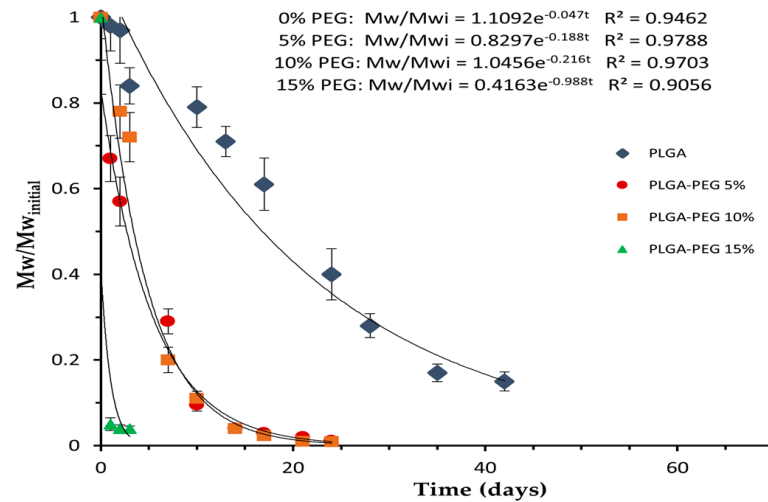


Figure 4. Normalized weight average molecular weight of PLGA, PLGA-5% PEG, PLGA-10% PEG and PLGA-15% PEG polymers in unloaded microspheres over 70 days. The solid lines represent exponential fits.

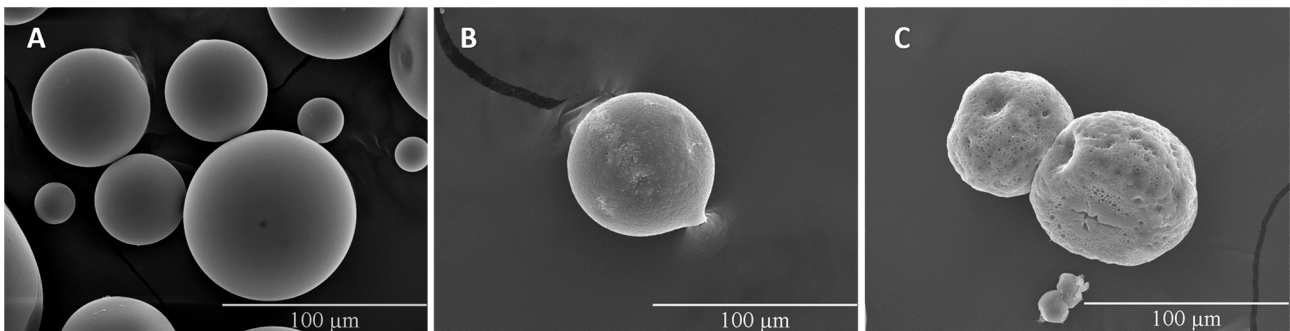


Figure 5. SEM images of ACM-loaded PLGA MP: (A) Initial; (B) 17 days; (C) 28 days after in vitro degradation. The scaling bars correspond to 100 µm.

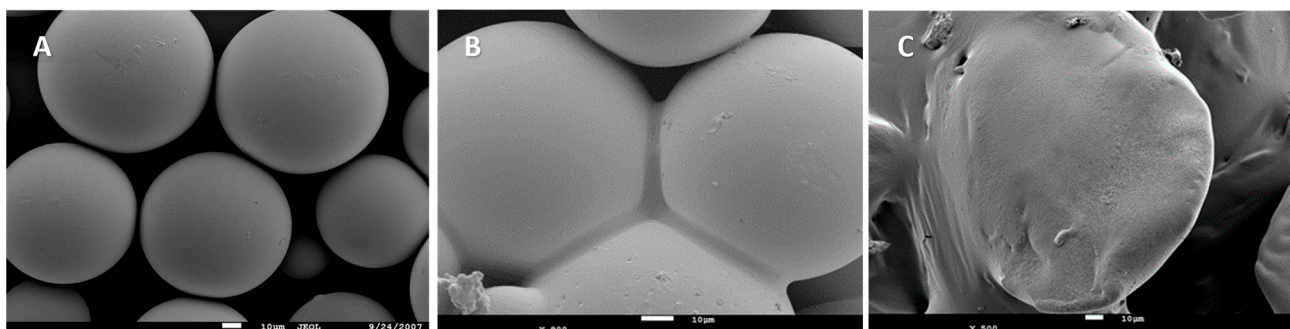


Figure 6. SEM images of PLGA-5% PEG microspheres: (A) Initial; (B) 10 days; (C) 17 days after in vitro degradation. The scaling bars correspond to 10 µm.

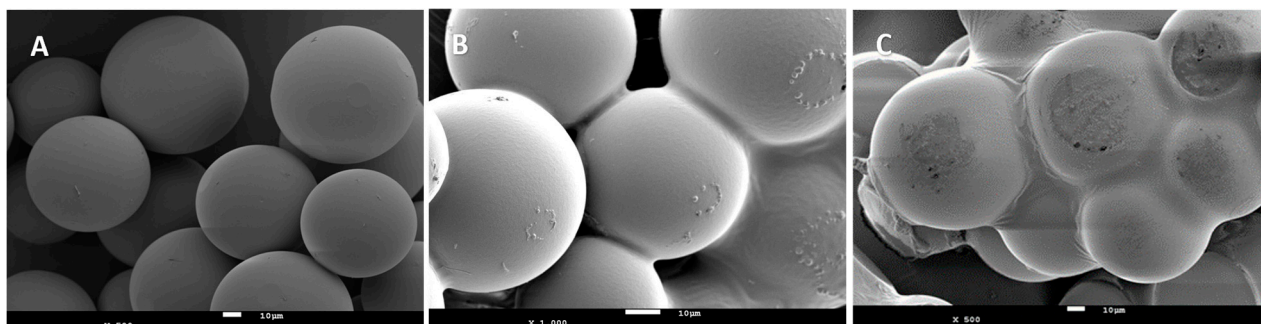


Figure 7. SEM images of PLGA-10% PEG microspheres: (A) Initial; (B) 10 days; (C) 17 days after in vitro degradation. The scaling bars correspond to 10 µm.

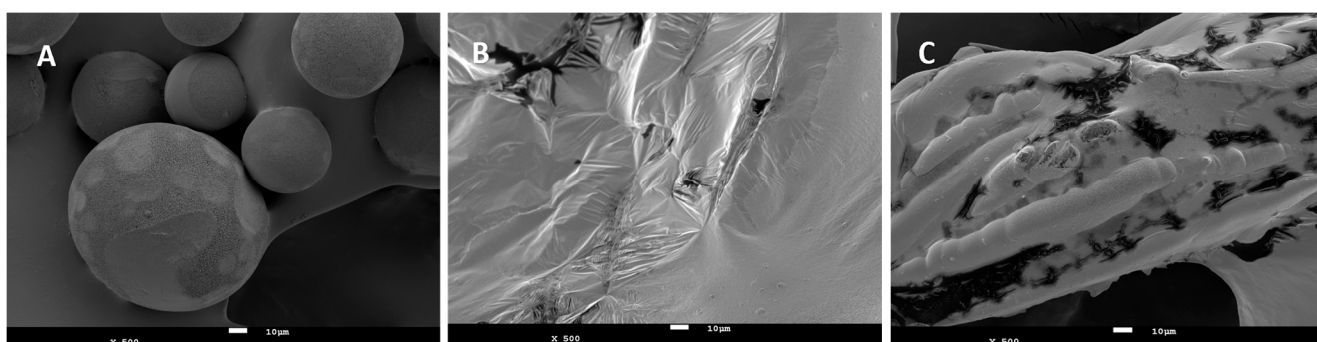


Figure 8. SEM images of PLGA-15% PEG microspheres: (A) Initial; (B) 1 day; (C) 3 days after in vitro degradation. The scaling bars correspond to 10 µm.

After 17 days, the microspheres containing 5% PEG no longer retained their spherical shape although some structural integrity remained, while those with 10% PEG had formed aggregates with a higher degree of coalescence. At this time, the molecular weights had decreased to 3% and 2% of their initial values for PLGA-5% PEG and PLGA-10% MP, respectively, reaching molecular weights of 18,000 Da and 16,000 Da, below the critical threshold of 20,000 Da identified by Spenlehauer et al. [41] as the point where PLGA systems begin to experience mass loss and accelerated erosion, while for PLGA MP the polymer molecular weight had decreased to 61% (54,000 Da). After approximately 20 days (20.7 days for 5%PEG and 19.9 days for 10% PEG), the molecular weights of the polymers in these MP reached 10,000 Da, a level never attained by pure PLGA MP.

The degradation study of PLGA-15% PEG MP, shown in Figure 8, indicates that within just one day, the particles lost their structural shape and present an irregular appearance, consistent with the 95% reduction in Mw observed in Figure 4. Additionally, the polymer Tg of 16.3 °C is significantly lower than the temperature used in the degradation test, which likely promoted the plastic deformation of the microspheres.

3.3. In Vitro Drug Release Study

To investigate the effect of PEG content in the polymer on the ACM release profile, in vitro release experiments from microspheres made of PLGA with various PEG contents were performed. The cumulative amount of ACM released with incubation time for microspheres of PLGA, PLGA-5% PEG, PLGA-10% PEG and PLGA-15% PEG in PBS buffer (pH 7.4) is shown in Figure 9. All microspheres of copolymer of PLGA containing PEG present higher release rates than PLGA microspheres and reached after 70 days a cumulative release value between 95% and 100% while for PLGA microspheres this value is 50%. This difference would be even more pronounced since the PLGA used has a much lower molecular weight than the PLGA-PEG polymers and higher release

rates have been reported for polymers with lower molecular weights [2,7,42]. All MP showed a triphasic release profile, similar to those reported in literature for PLGA-PEG MP [7,13,21,43]. The release profile began with an initial burst phase associated with the release of drug molecules located at or near the surface of the microspheres that diffuse out rapidly as water penetrates the polymer matrix. The PLGA-15% PEG MP gave the larger burst of 40%, versus 5% for PLGA MP. This phase is followed by a second, slower release phase, attributed to the gradual diffusion of drug, either through the denser polymer regions or through existing pores. In this phase, degradation of polymer chains occurs, preceding a faster release phase often linked to the onset of particles erosion [44]. These phases were found to vary significantly regarding quantity, duration and rate of drug released. PLGA-PEG MP present a shorter phase II than PLGA MP, with the duration of this phase decreasing as the PEG content in the polymer increased. This suggests that higher PEG contents accelerate the transition to the erosion-driven release phase. The onset of phase III release corresponds to the polymers reaching the aforementioned critical molecular weight threshold value of 20,000 Da. This occurred at different times for the polymers under study: 34 days for PLGA, 17 days for PLGA-5% PEG, 16.7 days for PLGA-10% PEG, and 2.5 days for PLGA-15% PEG. The fractional release data of ACM were fitted to the Corrigan model, a mechanistic model described by Equation (5), which incorporates contributions from both an initial first-order release phase and a polymer degradation release phase thus making it possible to describe the triphasic release profiles obtained.

$$\frac{M_t}{M_\infty} = F_b(1 - e^{-k_b t}) + (1 - F_b) \left(\frac{e^{k(t-t_{\max})}}{1 + e^{k(t-t_{\max})}} \right) \quad (5)$$

where M_t/M_∞ is the drug fraction released at time t , F_b is the total burst fraction at time infinity, k_b is the burst rate constant, t_{\max} is the time for maximum rate and k is the rate constant of the polymer degradation/erosion release phase [45].

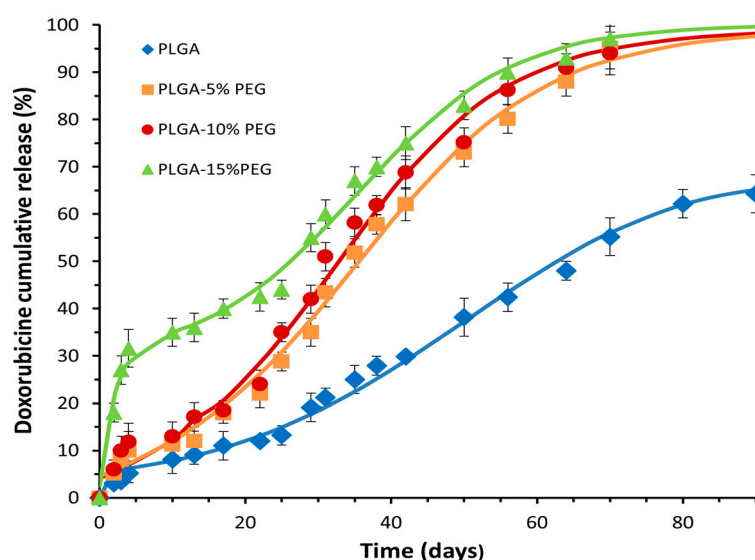


Figure 9. Cumulative ACM release from MP of PLGA-PEG with 5%, 10% and 15% of PEG. The lines represent the Corrigan model fitting (Equation (5)).

The drug release parameters estimated within a 95% confidence level, summarized in Table 2, provide a reasonably good fit across all sets, which can be confirmed by the R^2_{adj} and the MSC values obtained. One can see that F_b and K_b increase from 0.082 ± 0.021 to 0.288 ± 0.033 and from $0.012 \pm 0.004 \text{ day}^{-1}$ to $0.50 \pm 0.11 \text{ day}^{-1}$, respectively, as PEG content increases from 0% to 15%. The higher release fraction and release rate observed in the

burst phase are consistent with the presence of greater amounts of PEG in polymer chains. As previously discussed, the inclusion of PEG increases hydrophilicity and promotes water uptake, leading to pore formation and facilitating the escape of drug molecules during the early stages of release [12,46].

Table 2. Model parameters obtained from a nonlinear regression fit of the ACM release data from PLGA-PEG microspheres according to Equation (5).

PEG (%)	Fb	k_b (day ⁻¹)	t_{max} (day)	k (day ⁻¹)	R^2_{ad}	MSC
0	0.082 ± 0.021	0.012 ± 0.004	51.4 ± 1.2	0.054 ± 0.008	0.9966	4.144
5	0.112 ± 0.009	0.024 ± 0.010	36.1 ± 2.7	0.081 ± 0.006	0.9923	4.424
10	0.120 ± 0.008	0.025 ± 0.004	33.8 ± 0.6	0.091 ± 0.005	0.9906	4.443
15	0.288 ± 0.033	0.50 ± 0.11	35.4 ± 1.4	0.093 ± 0.006	0.9934	4.5695

It is a well-established fact that the transition of a polymer from the glassy to the rubbery state is accompanied by a considerable increase in permeability. In fact, PEG copolymers have a T_g close to or below 37 °C, which means that at the temperature at which the release study takes place, they are in the rubber state. The copolymer microspheres with the higher PEG content (15% PEG) have already released 30% of the drug content in 4 days. This might be due to the plastic deformation caused by the low polymer T_g , that can be observed in Figure 8B, where after one day the MP have completely lost their shape, leaving only a mass of polymer. In addition, this increment in polymer hydrophilicity also promoted a faster degradation of polymers and the subsequent solubilization and leaching out of the PEG component creating an increase in porosity and microspheres erosion, as explained before, which enhanced the release as well. This effect on the process is visible in the degradation/erosion control parameters values, t_{max} and k_{deg} , obtained, presented in Table 2. PLGA MP exhibited the longest time to reach the maximum drug release rate (t_{max}) indicating the most extended delay before the onset of the erosion-controlled release phase. Increasing the PEG content from 0% to 10% causes a decrease in t_{max} from 51.4 ± 1.2 to 33.8 ± 0.6 days although for a content of 15% a slight increase in this parameter is observed. Regarding the degradation rate constant, k increases from 0.054 ± 0.008 day⁻¹ to 0.093 ± 0.006 day⁻¹ with PEG content which is consistent with the results obtained in the degradation studies, as previously discussed. This fact shows that the behavior of the drugs release profile clearly depends on the polymer degradation as found by Corrigan and Li. Values of k in the same order of magnitude were obtained by Corrigan and Li with different molecules in PLGA NP [23] and Dunne et al. for pure PLGA NP [24]. Over time, the reduction in drug amount and the dissolution of the polymer chains with low molecular weights from the microspheres will result in a decline in the release rate of ACM.

4. Conclusions

Biodegradable microspheres composed of PLGA-PEG copolymers with 0%, 5%, 10%, and 15% PEG content, loaded with Aclacinomycin A, a low molecular weight drug, were prepared using the oil-in-water solvent evaporation technique. SEM micrographs revealed spherical microspheres with smooth surfaces and no visible pores across all formulations except for those with the highest PEG content (15%), which exhibited an irregular and porous surface. In vitro drug release studies demonstrated controlled ACM release over 70 days, following a triphasic release profile. Microspheres with higher PEG content displayed faster and more extensive ACM release due to increased hydrophilicity and potentially enhanced porosity. However, since porosity as well as mass loss were not assessed in this study, the lack of such data restricted our understanding of internal structure and erosion dynamics. Future investigations incorporating these measurements could provide

deeper insights into the release dynamics. The Corrigan model effectively described the drug release data, allowing the determination of burst release and degradation/erosion parameters. Increased PEG content led to a higher burst release, a shorter lag time before the degradation-controlled phase, as reflected by the time to maximum release (t_{max}), and an increase in the degradation/erosion rate (k). These findings demonstrate that the drug release profile can be effectively modified and controlled by adjusting the PEG content in the polymer matrix used for microsphere production. It is important to note that in vitro conditions do not fully replicate the complexity of in vivo environments, potentially limiting the extrapolation of findings to clinical applications. Future studies should focus on in vivo evaluations to validate the performance of these systems. Additionally, investigating a broader range of drugs could enhance the understanding and versatility of these microsphere formulations.

Author Contributions: Conceptualization, M.M.C. and A.M.R.; Data curation, M.M.C.; methodology, M.M.C. and A.M.R.; software, M.M.C.; formal analysis, M.M.C. and A.M.R.; investigation, M.S.C.; resources, M.M.C. and A.M.R.; writing—original draft preparation, M.S.C., M.M.C. and A.M.R.; writing—review and editing, M.M.C. and A.M.R.; supervision, M.M.C. and A.M.R.; project administration, M.M.C.; funding acquisition, M.M.C. All authors have read and agreed to the published version of the manuscript.

Funding: This work was supported by national funds from FCT—Fundação para a Ciência e a Tecnologia, Portugal, under projects [POCTI/EQU/46715/2002 from the QCA III/FEDER; PTDC/EQU/EPR/119631/2010, and Associated Laboratory for Green Chemistry (LAQV) of the Network of Chemistry and Technology (REQUIMTE)—LAQV/REQUIMTE (LA/P/0008/2020 DOI 10.54499/LA/P/0008/2020, UIDB/50006/2020 DOI 10.54499/UIDB/50006/2020 and UIDP/50006/2020 DOI 10.54499/UIDP/50006/2020)] and the research fellowship SFRH/BD/17224/2004.

Data Availability Statement: The original contributions presented in the study are included in the article, further inquiries can be directed to the corresponding author.

Acknowledgments: The authors acknowledge the Analytical services laboratory of REQUIMTE for the DSC results.

Conflicts of Interest: The authors declare no conflicts of interest.

References

1. Prajapati, V.D.; Jani, G.K.; Kapadia, J.R. Current Knowledge on Biodegradable Microspheres in Drug Delivery. *Expert Opin. Drug Deliv.* **2015**, *12*, 1283–1299. [[CrossRef](#)]
2. Freiberg, S.; Zhu, X.X. Polymer Microspheres for Controlled Drug Release. *Int. J. Pharm.* **2004**, *282*, 1–18. [[CrossRef](#)] [[PubMed](#)]
3. Anderson, J.M.; Shive, M.S. Biodegradation and Biocompatibility of PLA and PLGA Microspheres. *Adv. Drug Deliv. Rev.* **1997**, *28*, 5–24. [[CrossRef](#)]
4. Jain, R.A. The Manufacturing Techniques of Various Drug Loaded Biodegradable Poly(Lactide-Co-Glycolide) (PLGA) Devices. *Biomaterials* **2000**, *21*, 2475–2490. [[CrossRef](#)]
5. Peppas, N.A.; Huang, Y.; Torres-Lugo, M.; Ward, J.H.; Zhang, J. Physicochemical Foundations and Structural Design of Hydrogels in Medicine and Biology. *Annu. Rev. Biomed. Eng.* **2000**, *2*, 9–27. [[CrossRef](#)] [[PubMed](#)]
6. Proikakis, C.S.; Tarantili, P.A.; Andreopoulos, A.G. The Role of Polymer/Drug Interactions on Sustained Release from Poly(DL-Lactic Acid) Tablets. *Eur. Polym. J.* **2006**, *42*, 3269–3276. [[CrossRef](#)]
7. Raman, C.; Berkland, C.; Kim, K.K.; Pack, D.W. Modeling Small-Molecule Release from PLG Microspheres: Effects of Polymer Degradation and Nonuniform Drug Distribution. *J. Control. Release* **2005**, *103*, 149–158. [[CrossRef](#)]
8. Tuncay, M.; Calis, S.; Kas, H.S.; Ercan, M.T.; Peksoy, I.; Hincal, A.A. Diclofenac Sodium Incorporated PLGA (50:50) Microspheres: Formulation Considerations and In Vitro: In Vivo Evaluation. *Int. J. Pharm.* **2000**, *195*, 179–188. [[CrossRef](#)] [[PubMed](#)]
9. Ford Versypt, A.N.; Pack, D.W.; Braatz, R.D. Mathematical Modeling of Drug Delivery from Autocatalytically Degradable PLGA Microspheres—A Review. *J. Control. Release* **2013**, *165*, 29–37. [[CrossRef](#)]

10. Mallardé, D.; Boutignon, F.; Moine, F.; Pinchard, A.; Coubard, J.; Petavy, F. PLGA-PEG Microspheres of Teverelix: Influence of Polymer Type on Microsphere Characteristics and on Teverelix In Vitro Release. *Int. J. Pharm.* **2003**, *261*, 69–80. [[CrossRef](#)] [[PubMed](#)]
11. Li, X.; Deng, X.; Yuan, M.; Xiong, C.; Huang, Z.; Zhang, Y.; Jia, W.; Gao, Y. In Vitro Degradation and Release Profiles of Poly-DL-Lactide-Poly(Ethylene Glycol) Microspheres with Entrapped Proteins. *J. Appl. Polym. Sci.* **2000**, *78*, 140–148. [[CrossRef](#)]
12. Ruan, G.; Feng, S.S. Preparation and Characterization of Poly(Lactic Acid)-Poly(Ethylene Glycol)-Poly(Lactic Acid) (PLA-PEG-PLA) Microspheres for Controlled Release of Paclitaxel. *Biomaterials* **2003**, *24*, 5037–5044. [[CrossRef](#)]
13. Lochmann, A.; Hagen, N.; Von Einem, S.; Schwarz, E.; Mäder, K. The Influence of Covalently Linked and Free Polyethylene Glycol on the Structural and Release Properties of rhBMP-2 Loaded Microspheres. *J. Control. Release* **2010**, *147*, 92–100. [[CrossRef](#)]
14. Agrawal, S.K.; Sanabria-DeLong, N.; Coburn, J.M.; Tew, G.N.; Bhatia, S.R. Novel Drug Release Profiles from Micellar Solutions of PLA-PEG-PLA Triblock Copolymers. *J. Control. Release* **2006**, *112*, 64–71. [[CrossRef](#)]
15. Zhang, K.; Tang, X.; Zhang, J.; Lu, W.; Lin, X.; Zhang, Y.; He, H. PEG–PLGA Copolymers: Their Structure and Structure-Influenced Drug Delivery Applications. *J. Control. Release* **2014**, *183*, 77–86. [[CrossRef](#)]
16. Cardoso, M.M.; Peça, I.N.; Bicho, A. Impact of PEG Content on Doxorubicin Release from PLGA-co-PEG Nanoparticles. *Materials* **2024**, *17*, 3544. [[CrossRef](#)]
17. Essa, S.; Rabanel, J.M.; Hildgen, P. Effect of Polyethylene Glycol (PEG) Chain Organization on the Physicochemical Properties of Poly(D,L-lactide) (PLA)-Based Nanoparticles. *Eur. J. Pharm. Biopharm.* **2010**, *75*, 96–106. [[CrossRef](#)] [[PubMed](#)]
18. Mäder, K.; Bittner, B.; Li, Y.; Wohlauf, W.; Kissel, T. Monitoring Microviscosity and Microacidity of the Albumin Microenvironment Inside Degrading Microparticles from Poly(Lactide-co-Glycolide) (PLG) or ABA-Triblock Polymers Containing Hydrophobic Poly(Lactide-co-Glycolide) A Blocks and Hydrophilic Poly(Ethylene Oxide) B Blocks. *Pharm. Res.* **1998**, *15*, 787–793. [[CrossRef](#)]
19. Yeh, M.K.; Jenkins, P.G.; Davis, S.S.; Coombes, A.G.A. Improving the Delivery Capacity of Microparticle Systems Using Blends of Poly(DL-lactide-co-glycolide) and Poly(Ethylene Glycol). *J. Control. Release* **1995**, *37*, 1–9. [[CrossRef](#)]
20. LaPorte, R.J. *Hydrophilic Polymer Coatings for Medical Devices: Structure/Properties, Development, Manufacture, and Applications*; Technomic Publishing Company: Lancaster, PA, USA, 1997. [[CrossRef](#)]
21. Ramtoola, Z.; Corrigan, O.I.; Barrett, C.J. Release Kinetics of Fluphenazine from Biodegradable Microspheres. *J. Microencapsul.* **1992**, *9*, 415–423. [[CrossRef](#)]
22. Corrigan, O.I.; Heelan, B.A. Characterization of Drug Release from Diltiazem-Loaded Polylactide Microspheres Prepared Using Sodium Caseinate and Whey Protein as Emulsifying Agents. *J. Microencapsul.* **2001**, *18*, 335–345. [[CrossRef](#)] [[PubMed](#)]
23. Corrigan, O.I.; Li, X. Quantifying Drug Release from PLGA Nanoparticulates. *Eur. J. Pharm. Sci.* **2009**, *37*, 477–485. [[CrossRef](#)] [[PubMed](#)]
24. Dunne, M.; Corrigan, O.I.; Ramtoola, Z. Influence of Particle Size and Dissolution Conditions on the Degradation Properties of Polylactide-Co-Glycolide Particles. *Biomaterials* **2000**, *21*, 1659–1668. [[CrossRef](#)]
25. Thong, N.G.; Hanh, V.T.H.; Bui, T.T.; Nguyen, V.M.; Le, T.P.H.; Tran, N.T.H. Investigation on Modeling and Correlating Drug Release Profiles in the Accelerated and Real-Time Conditions to Formulate Leuprolide Acetate-Loaded Biodegradable Microspheres. *J. Drug Deliv. Sci. Technol.* **2023**, *86*, 104529. [[CrossRef](#)]
26. Buske, J.; König, C.; Bassarab, S.; Lamla, M.; Schaper, A.K.; Betz, O.; Goepferich, A. Influence of PEG in PEG–PLGA Microspheres on Particle Properties and Protein Release. *Eur. J. Pharm. Biopharm.* **2012**, *81*, 57–63. [[CrossRef](#)] [[PubMed](#)]
27. De Souza, L.E.; Eckenstaler, R.; Syrowatka, F.; Beck-Broichsitter, M.; Benndorf, R.A.; Mäder, K. Has PEG-PLGA Advantages for the Delivery of Hydrophobic Drugs? Risperidone as an Example. *J. Drug Deliv. Sci. Technol.* **2021**, *61*, 102239. [[CrossRef](#)]
28. Monneret, C. Recent Developments in the Field of Antitumor Anthracyclines. *Eur. J. Med. Chem.* **2001**, *36*, 483–493. [[CrossRef](#)] [[PubMed](#)]
29. Wang, J.; Maitani, Y.; Takayama, K. Antitumor Effects and Pharmacokinetics of Aclacinomycin A Carried by Injectable Emulsions Composed of Vitamin E, Cholesterol, and PEG-Lipid. *J. Pharm. Sci.* **2002**, *91*, 1128–1134. [[CrossRef](#)]
30. Murzyn, A.; Orzeł, J.; Obajtek, N.; Mróz, A.; Miodowska, D.; Bojdo, P.; Gąsioriewicz, B.; Koczurkiewicz-Adamczyk, P.; Piska, K.; Pękala, E. Aclarubicin: Contemporary Insights into Its Mechanism of Action, Toxicity, Pharmacokinetics, and Clinical Standing. *Cancer Chemother. Pharmacol.* **2024**, *94*, 123–139. [[CrossRef](#)]
31. PerkinElmer. Application Note: Tg and Melting Point of a Series of Polyethylene Glycol Standards with Different Molecular Weights. 2012. Available online: https://resources.perkinelmer.com/lab-solutions/resources/docs/APP_TGA_PEGStandards_012.pdf (accessed on 15 July 2024).
32. Chiba, M.; Hanes, J.; Langer, R. Controlled Protein Delivery from Biodegradable Tyrosine-Containing Poly(anhydride-co-imide) Microspheres. *Biomaterials* **1997**, *18*, 893–901. [[CrossRef](#)]
33. Gupte, A.; Ciftici, K. Formulation and Characterization of Paclitaxel, 5-FU, and Paclitaxel + 5-FU Microspheres. *Int. J. Pharm.* **2004**, *276*, 93–106. [[CrossRef](#)] [[PubMed](#)]

34. Khan, I.; Gothwal, A.; Sharma, A.K.; Qayum, A.; Singh, S.K.; Gupta, U. Biodegradable Nano-Architectural PEGylated Approach for the Improved Stability and Anticancer Efficacy of Bendamustine. *Int. J. Biol. Macromol.* **2016**, *92*, 1242–1251. [[CrossRef](#)] [[PubMed](#)]
35. Siepmann, J.; Elkharraz, K.; Siepmann, F.; Klose, D. How Autocatalysis Accelerates Drug Release from PLGA-Based Microparticles: A Quantitative Treatment. *Biomacromolecules* **2005**, *6*, 2312–2319. [[CrossRef](#)] [[PubMed](#)]
36. Ding, A.G.; Schwendeman, S.P. Acidic Microclimate pH Distribution in PLGA Microspheres Monitored by Confocal Laser Scanning Microscopy. *Pharm. Res.* **2008**, *25*, 2041–2052. [[CrossRef](#)] [[PubMed](#)]
37. Mauduit, J.; Bukh, N.; Vert, M. Gentamycin/Poly(Lactic Acid) Blends Aimed at Sustained Release Local Antibiotic Therapy Administered Per-Operatively. I. The Case of Gentamycin Base and Gentamycin Sulfate in Poly(DL-Lactic Acid) Oligomers. *J. Control. Release* **1993**, *23*, 209–220. [[CrossRef](#)]
38. Faisant, N.; Siepmann, J.; Benoit, J.P. PLGA-Based Microparticles: Elucidation of Mechanisms and a New, Simple Mathematical Model Quantifying Drug Release. *Eur. J. Pharm. Sci.* **2002**, *15*, 355–366. [[CrossRef](#)]
39. Park, T.G. Degradation of Poly(D,L-Lactic Acid) Microspheres: Effect of Molecular Weight. *J. Control. Release* **1994**, *30*, 161–173. [[CrossRef](#)]
40. Heller, J.; Penhale, D.W.; Fritzinger, B.K.; Ng, S.Y. The Effect of Copolymerized 9,10-Dihydroxystearic Acid on Erosion Rates of Poly(ortho esters) and Its Use in the Delivery of Levonorgestrel. *J. Control. Release* **1987**, *5*, 173–177. [[CrossRef](#)]
41. Spenlehauer, G.; Vert, M.; Benoit, J.P.; Boddart, A. In Vitro and In Vivo Degradation of Poly(DL-Lactide/Glycolide) Type Microspheres Made by Solvent Evaporation Method. *Biomaterials* **1989**, *10*, 557–563. [[CrossRef](#)]
42. Charlier, A.; Leclerc, B.; Couarraze, G. Release of Mifepristone from Biodegradable Matrices: Experimental and Theoretical Evaluations. *Int. J. Pharm.* **2000**, *200*, 115–120. [[CrossRef](#)] [[PubMed](#)]
43. Puebla, P.; Pastoriza, P.; Barcia, E.; Fernández-Carballido, A. PEG-Derivative Effectively Modifies the Characteristics of Indomethacin-PLGA Microspheres Destined to Intra-Articular Administration. *J. Microencapsul.* **2005**, *22*, 793–808. [[CrossRef](#)] [[PubMed](#)]
44. Fredenberg, S.; Wahlgren, M.; Reslow, M.; Axelsson, A. The Mechanisms of Drug Release in Poly(Lactic-Co-Glycolic Acid)-Based Drug Delivery Systems—A Review. *Int. J. Pharm.* **2011**, *415*, 34–52. [[CrossRef](#)] [[PubMed](#)]
45. Gallagher, K.M.; Corrigan, O.I. Mechanistic Aspects of the Release of Levamisole Hydrochloride from Biodegradable Polymers. *J. Control. Release* **2000**, *69*, 261–272. [[CrossRef](#)]
46. Blanco-Prieto, M.J.; Besseghir, K.; Zerbe, O.; Andris, D.; Orsolini, P.; Gander, B.; Doelker, E. In Vitro and In Vivo Evaluation of a Somatostatin Analogue Released from PLGA Microspheres. *J. Control. Release* **2000**, *67*, 19–28. [[CrossRef](#)]

Disclaimer/Publisher’s Note: The statements, opinions and data contained in all publications are solely those of the individual author(s) and contributor(s) and not of MDPI and/or the editor(s). MDPI and/or the editor(s) disclaim responsibility for any injury to people or property resulting from any ideas, methods, instructions or products referred to in the content.